

Gapless chirality liquid with symmetry-protected edge spins

Shunsuke C. Furuya¹ and Katsuhiko Morita²

¹*Department of Basic Science, University of Tokyo, Meguro, Tokyo 153-8902, Japan*

²*Department of Physics, Faculty of Science and Technology,
Tokyo University of Science, Chiba 278-8510, Japan*

(Dated: July 7, 2022)

We report that a spin-1/2 tetrahedral Heisenberg chain realizes a gapless symmetry-protected topological (gSPT) phase characterized by the coexistence of the Tomonaga-Luttinger-liquid criticality due to chirality degrees of freedom and the symmetry-protected edge state due to spin degrees of freedom. This gSPT phase has an interesting feature that no symmetry forbids the trivial spin gap opening but a discrete symmetry, $\mathbb{Z}_3 \times \mathbb{Z}_2^T$, forbids the unique gapped ground state. In the first part of the paper, we numerically show the coexistence of a critical entanglement entropy and a nontrivially degenerate entanglement spectrum based on the density-matrix renormalization group (DMRG) method. Next, we clarify that chirality degrees of freedom form the Tomonaga-Luttinger liquid while spin degrees of freedom form the spin-1 Haldane state based on a degenerate perturbation theory. Last but not least, we discuss the Lieb-Schultz-Mattis-type ingappability in the gSPT phase, using a local \mathbb{Z}_3 rotation. We can thus characterize our gSPT phase as a symmetry-protected critical phase protected by the \mathbb{Z}_3 on-site symmetry, the \mathbb{Z}_2^T time-reversal symmetry, the lattice translation symmetry, and the U(1) spin-rotation symmetry.

I. INTRODUCTION

Topological phases of matter now became a major research subject of condensed matter physics. Historically, researches on topological phases initially covered free fermion systems [1–3] and were later extended to strongly interacting systems. Symmetry protected topological (SPT) phases are one of the best studied topological phases in strongly interacting quantum many-body systems [4, 5]. The (gapped) SPT phase is characterized as a quantum phase that has a unique gapped ground state with a short-range entanglement protected by symmetries.

Recently, gapless topological phases have drawn intensive attention [6–13]. Dirac and Weyl semimetals are their good examples in noninteracting or weakly interacting fermion systems [6]. Naturally, people are giving their attention to gapless SPT (gSPT) phases in strongly interacting quantum many-body systems to get a deeper insight into topological phases of matter [7–13]. A naive definition of the gSPT phase is a gapless phase with a symmetry-protected entanglement.

However, we need careful considerations on the symmetry protection of the gSPT phase. The symmetry protection of the gSPT phase has two meanings: the symmetry protection of the edge state and the symmetry protection of gapless low-energy states in bulk. The symmetry protection in the former sense is nontrivial in the gSPT phase because of the absence of the excitation gap in bulk. The bulk gap is a precondition for the symmetry protection of the gapped SPT phase. The symmetry protection in the latter sense is also quite nontrivial. This symmetry protection is defined as the prohibition of any trivial opening of the bulk gap [14]. Here, we mean by trivial that the gap opens without any spontaneous symmetry breaking. The impossibility of the trivial gap opening is also called ingappability [15]. The ingappabil-

ity guarantees that the gSPT phase indeed qualifies as a phase of matter distinct from the other phases.

In this paper, we report a novel gSPT phase in geometrically frustrated quantum spin chains [Fig. 1 (a)] and discuss its symmetry protection in both senses. This gSPT phase hosts a critical chirality liquid with a symmetry-protected edge state. The tetrahedral spin chain can trivially open a spin gap because the unit cell contains a tetrahedron of four localized spins [Fig. 1 (a)]. Concerning the spin degrees of freedom, the ground state of this system looks like a valence-bond solid (VBS) state with a short-range entanglement. This gSPT phase hosts gapless low-energy excitations originating from chirality degrees of freedom without interfering the VBS texture.

We organize this paper as follows. Section II defines our model. We numerically investigate the model in Sec. III, where we confirm that the model indeed has the gSPT phase from the entanglement point of view. Section IV discusses the gSPT phase with the degenerate perturbation theory. The perturbation theory allows us to explicitly write down the low-energy effective Hamiltonian. The effective Hamiltonian clarifies that the gSPT phase in our system is the chirality liquid with symmetry-protected edge spins. Based on the results in Sec. IV, we discuss the ingappability of the gSPT phase in Sec. V. Finally, we summarize the paper in Sec. VI.

II. MODEL

Our model has the following Hamiltonian under the periodic boundary condition (PBC):

$$\mathcal{H} = J \sum_{r=1}^L (\mathbf{S}_{r,1} \cdot \mathbf{S}_{r,2} + \mathbf{S}_{r,2} \cdot \mathbf{S}_{r,3} + \mathbf{S}_{r,3} \cdot \mathbf{S}_{r,1})$$

$$\begin{aligned}
& + \alpha J \sum_{j=1}^L \mathbf{S}_{r,4} \cdot \mathbf{T}_r \\
& + J_t \sum_{r=1}^L \mathbf{S}_{r,4} \cdot \mathbf{T}_{r+1} + J_\ell \sum_{r=1}^L \sum_{n=1}^3 \mathbf{S}_{r,n} \cdot \mathbf{S}_{r+1,n}, \quad (1)
\end{aligned}$$

where $\mathbf{S}_{r,n}$ is an $S = 1/2$ localized spin at the n th vertex of the r th tetrahedron [Figs. 1 (a) and (b)] and $\mathbf{T}_r = \sum_{n=1}^3 \mathbf{S}_{r,n}$ is the total spin of the base triangle of the tetrahedron. The tetrahedral spin chain (1) contains $4L$ spins, where we call L a system length.

Three exchange couplings J , J_t , and J_ℓ are all positive (i.e., antiferromagnetic). We limit the dimensionless parameter α to $\alpha < 0$ so that each tetrahedron has three antiferromagnetic J bonds in the base triangle and three ferromagnetic αJ bonds that bridge the base triangle with the top of the tetrahedron [Fig. 1 (b)]. Throughout this paper, we assume $\max\{J_\ell, J_t\} \ll J$.

III. NUMERICAL RESULTS

Let us numerically investigate the tetrahedral spin chain (1) to get insight into its quantum phases. In this section, we fix $J_t/J = 0.2$ and $J_\ell/J = 0.1$ and vary α and the system length L . Our calculations are based on the density-matrix renormalization group (DMRG) method with the open boundary condition (OBC).

The ground-state phase diagram $-\infty < \alpha < 0$ contains two phases I and II separated by a quantum phase transition point $\alpha = \alpha_c$. Let us start with locating the phase transition point. Figure 1 (c) shows a second derivative $-d^2 E_{\text{GS}}/d\alpha^2$ of the GS energy for $-4 < \alpha < 0$, where we took $L = 30$. The derivative shows a singular increase at $\alpha = \alpha_c \approx -0.27$. This value separates two phases, I for $\alpha_c < \alpha < 0$ and II for $\alpha < \alpha_c$. We can identify the phase I and II as the gSPT phase and a spin-2 Haldane phase, respectively. In what follows, we amass evidences of this identification of quantum phases.

A. Phase I: gSPT phase

We numerically confirm that the phase I is the gSPT phase in two stages. First, we show that the phase I is a critical phase with gapless excited states. Second, we show that the ground state in the phase I has a nontrivial short-range entanglement.

1. Entanglement entropy

Let us show that the phase I is a critical phase described by a conformal field theory (CFT) with a central charge $c = 1$. Figure 2 shows the entanglement entropy S_E at $\alpha = -1.2$, where we take the system length $L = 200$. In the calculations of the entanglement, we

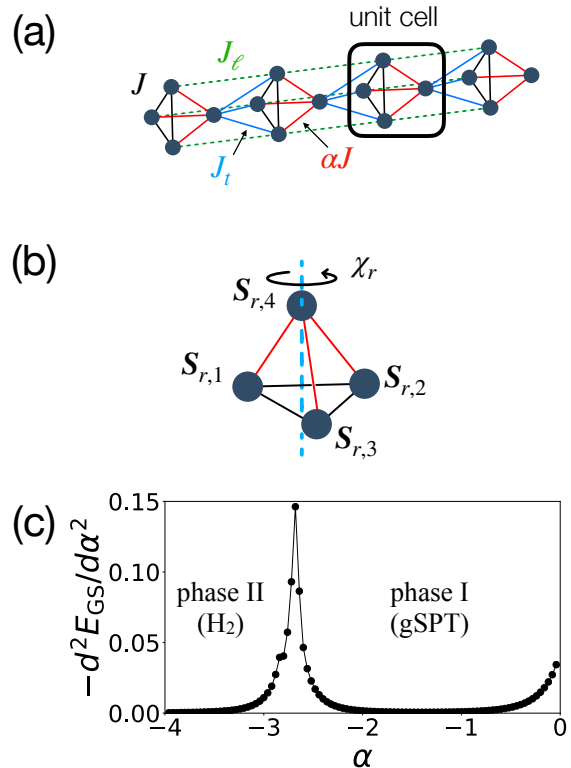


FIG. 1. (a) Tetrahedral spin chain. The unit cell contains one tetrahedron with three antiferromagnetic $J > 0$ and three ferromagnetic $\alpha J < 0$ bonds. (b) Single tetrahedron with base triangle formed by $\mathbf{S}_{r,n}$ with $n = 1, 2, 3$ and vertex $\mathbf{S}_{r,4}$. The solid curve around the dashed line piercing the base triangle and the vertex $\mathbf{S}_{r,4}$ depict the chirality $\chi_r = \pm 1$ of the tetrahedron. (c) Second derivative $-d^2 E_{\text{GS}}/d\alpha^2$ of GS energy calculated by using DMRG with parameters $L = 30$, $J_t/J = 0.2$, $J_\ell/J = 0.1$. The derivative shows a singularity at $\alpha = \alpha_c \approx -0.27$. The point $\alpha = \alpha_c$ defines phase I and II. As we show later, we identify the phases I ($\alpha_c < \alpha < 0$) and II ($\alpha < \alpha_c$) as the gSPT phase and the spin-2 Haldane phase (H₂), respectively.

fix the total magnetization to $\langle S_{\text{tot}}^z \rangle = 1$ to minimize the boundary effects into the entanglement entropy. We confirmed that the ground-state energies in $\langle S_{\text{tot}}^z \rangle = 1, 0, -1$ sectors are well degenerate.

If the conformal symmetry emerges at low energies, the entanglement entropy of the ground state with the OBC follows a so-called Calabrese-Cardy formula [16],

$$S_E = \frac{c}{6} \ln \left[\frac{2L}{\pi} \sin \left(\frac{\pi r}{L} \right) \right] + \ln g + a, \quad (2)$$

with a constant a . The site $r = 1, 2, \dots, L - 1$ in Eq. (2) represents the bond between the r th and $(r+1)$ th tetrahedra. Note that we included a boundary entropy $\ln g$ [17, 18] in Eq. (2). The boundary entropy shows the following site dependence

$$\ln g = b(-1)^x \left[\frac{L}{\pi} \sin \left(\frac{\pi r}{L} \right) \right]^{-1}. \quad (3)$$

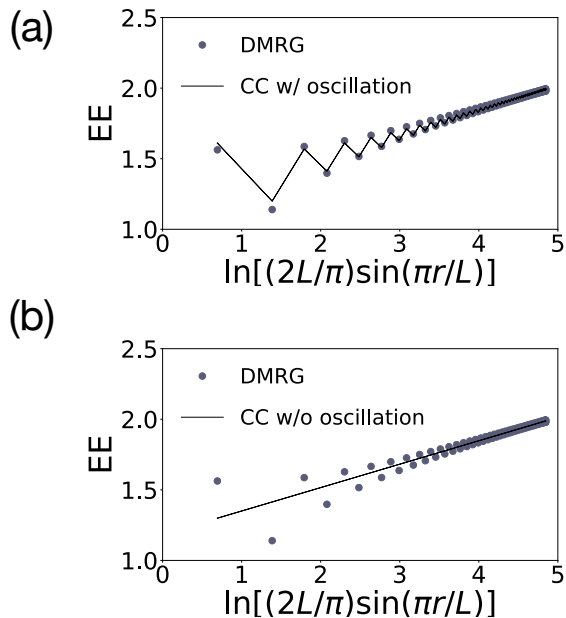


FIG. 2. Entanglement entropy in gSPT phase. In both panels, gray balls are DMRG data with $L = 200$, $J_t/J = 0.2$, $J_\ell/J = 0.1$, and $\alpha = -1.2$. Solid curves are fitting results of the DMRG data with the Calabrese-Cardy formula (2) (a) with and (b) without the oscillating term (3) originating from boundary degrees of freedom. Both give the consistent fitting result of the central charge c close to $c = 1$. The former gives $c \approx 1.07$ and the latter gives $c \approx 0.995$.

In the spin-1/2 XXZ chain, the constant b takes a universal value $b = -1$ [18]. Considering the complexity of our system, we regard b as a free parameter and determine a , b , and c by comparing Eq. (2) with the DMRG data. In Fig. 2 (a), we fit Eq. (2) with the DMRG data by changing a , b , and c . We then obtain optimal values $(a, b, c) = (1.13124304, -0.35605475, 1.06698522)$. The central charge $c \approx 1.07$ is close to the value $c = 1$. The Tomonaga-Luttinger liquid (TLL) is the most likely candidate of the $c = 1$ CFT in quantum spin chains [19].

We can take an alternative approach to estimate the central charge c . That is, we ignore the data close to boundary and fit the DMRG data with the Calabrese-Cardy formula (2) without the oscillating boundary term (i.e., $b = 0$). In Fig. 2 (b), we discarded the first six data $r = 1, 2, \dots, 6$ and fit the remaining data with Eq. (2) with $b = 0$. Note that we plotted the DMRG data for $r = 1, 2, \dots, L/2$ in Fig. 2 because of the reflection symmetry $r \rightarrow L - r$ of the tetrahedral spin chain with the OBC. We then obtain $(a, c) = (1.18421471, 0.99530899)$. Again, we find the central charge $c \approx 0.995$ close to $c = 1$. Therefore, we conclude that the phase I is described by the $c = 1$ CFT.

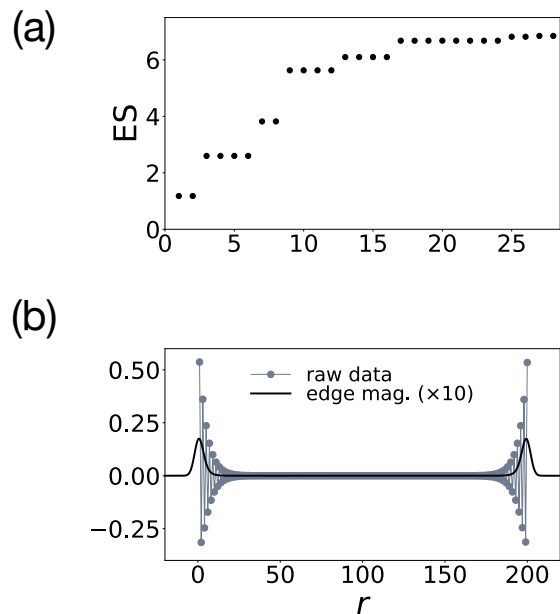


FIG. 3. (a) Entanglement spectrum $\{\mu_i = -\ln(\lambda_i^2)\}_{i=1,2,\dots}$ at central bond in gSPT phase ($\alpha = -1.2$ and $L = 200$). λ_i denotes the Schmidt eigenvalue. We label λ_i with i in ascending order of μ_i . The horizontal axes show i and λ_i , respectively. We can find clear even-fold degeneracy of the entanglement spectrum. (b) Magnetization density $S_{r,\text{tot}}^z$ (gray balls) and edge magnetization $m^z(r)$ (solid curve) plotted with respect to r . We derive the latter from the former through a Gaussian convolution [20]. Both quantities show the growth of the nonzero magnetization at both edges of the chain $r = 1, L$. In particular, the latter shows a fractional quantization $M_{\text{left}}^z = M_{\text{right}}^z = 1/2$, an evidence of the fractional $S = 1/2$ edge spin of the AKLT state (see the main text.).

2. Entanglement spectrum and edge magnetization

The phase I has yet another interesting property about the entanglement. Figure 3 (a) shows the entanglement spectrum $\{\mu_i\}_{i=1,2,\dots}$ at $\alpha = -1.2$ with $L = 200$ in the $\langle S_{\text{tot}}^z \rangle = 1$ sector. The eigenvalue $\mu_i = -\ln(\lambda_i^2)$ is obtained from the Schmidt eigenvalue λ_i . We measured the entanglement at the center bond $r = L/2$ of the spin chain. The entanglement spectrum exhibits a clear even-fold degeneracy. The even-fold degeneracy implies that the ground state is a short-range-entangled VBS state similar to a spin-1 Haldane state.

The spin-1 Haldane state is the unique gapped ground state of the spin-1 Heisenberg antiferromagnetic chain with the PBC [21–23] and one of the best-known gapped SPT states [24–26]. According to the bulk-edge correspondence in the gapped SPT phase, the nontrivial entanglement spectrum indicates the existence of nontrivial edge states. Indeed, it is well known that the spin-1 Haldane state with the OBC hosts two symmetry-protected edge spins with the fractional spin quantum

number $S = 1/2$ [27].

The ground state in our gSPT phase also shows edge states akin to the fractional $S = 1/2$ edge state of the spin-1 Haldane state. Gray balls in Fig. 3 (b) represent the spatial distribution $\langle S_r^z \rangle$ of the magnetization per tetrahedron:

$$\langle S_r^z \rangle = \sum_{n=1}^4 \langle S_{r,n}^z \rangle. \quad (4)$$

The magnetization density (4) is nonzero around the edges of the chain while it is flatly zero deep inside the bulk.

We can show that the nonzero magnetization localized around the edges indeed represents the fractional $S = 1/2$ edge state as follows. Recently, a magnetic analog of the bulk electric polarization was proposed to characterize gapped quantum phases [20]. This magnetic analog is called an edge (corner) magnetization in one-dimensional (two- or higher-dimensional, respectively) spin systems. While Ref. [20] focused on topologically trivial phases, later, the edge magnetization turned out to also be relevant to SPT phases in spin chains. In fact, one of the authors showed that the edge magnetizations M_{left}^z and M_{right}^z in the spin-1 Haldane state originate from the fractional $S = 1/2$ edge spin [28]. Here, we denote the edge magnetizations on the left and right edges of the spin chain as M_{left}^z and M_{right}^z , respectively. The edge magnetizations in the spin-1 Haldane state are quantized as $M_{\text{left}}^z = \pm 1/2$ and $M_{\text{right}}^z = \pm 1/2$. To fix the sign of the edge magnetization, we performed DMRG calculations in the $\langle S_{\text{tot}}^z \rangle = 1$ sector.

We define the edge magnetizations M_{left}^z and M_{right}^z as follows. First, we take a Gaussian convolution of the magnetization per tetrahedron $\langle S_r^z \rangle$:

$$m^z(r) = \sum_{r'=1}^L g(r-r') \langle S_{r'}^z \rangle, \quad (5)$$

where $g(r)$ is a normalized Gaussian function parameterized with a positive constant λ :

$$g(r) = \frac{1}{\sqrt{2\pi\lambda^2}} \exp\left(-\frac{r^2}{2\lambda^2}\right). \quad (6)$$

The Gaussian convolution (5) smooths the raw data of $\langle S_r^z \rangle$. The solid curve of Fig. 3 (b) depicts $m^z(r)$ with $\lambda = 5$. The value of $\lambda > 0$ can be arbitrary.

Next, based on the smoothed magnetization density (5), we define the edge magnetization M_{left}^z (M_{right}^z) on the left (right) as an area swept by $m^z(r)$ when r runs over the left (right, respectively) half of the system:

$$M_{\text{left}}^z = \int_{-\infty}^{(L+1)/2} dr m^z(r), \quad M_{\text{right}}^z = \int_{(L+1)/2}^{\infty} dr m^z(r). \quad (7)$$

By construction, the sum of the edge magnetizations gives the total magnetization $M_{\text{left}}^z + M_{\text{right}}^z = \langle S_{\text{tot}}^z \rangle$.

The DMRG raw data of Fig. 3 (b) gives

$$(M_{\text{left}}^z, M_{\text{right}}^z) = (0.4999999, 0.5000001). \quad (8)$$

The edge magnetizations are well quantized to $M_{\text{left}}^z = M_{\text{right}}^z = 1/2$. We thus conclude that the phase I is the gSPT phase with the $c = 1$ CFT criticality and the symmetry-protected $S = 1/2$ edge spin.

B. Phase II: spin-2 Haldane phase

We now give our attention to the phase II. Figure 4 shows (a) the entanglement entropy, (b) the entanglement spectrum, and (c) the edge magnetization at $\alpha = -3.5$ with $L = 350$ in the $\langle S_{\text{tot}}^z \rangle = 2$ sector. We obtained the solid curve of Fig. 4 (a) by fitting the numerically obtained entanglement entropy in a range $30 < r < L$ with the Calabresse-Cardy formula (2) with $b = 0$. We then obtained the result $(a, c) = (1.51995057, 0.17321388)$. However, the Calabresse-Cardy formula (2) does not fit well with the numerically obtained entanglement entropy in the range $30 < r < L$. Hence, the phase II is not critical and highly likely to be weakly gapped. The entanglement spectrum of Fig. 4 (b) indicates that the phase II is topologically trivial. Finally, Fig. 4 (c) shows the quantized edge magnetizations $(M_{\text{left}}^z, M_{\text{right}}^z) = (0.99999, 1.00001)$. The DMRG calculations in Fig. 4 are done under a constraint $\langle S_{\text{tot}}^z \rangle = 2$ to make M_{left}^z and M_{right}^z positive. We confirmed that the ground-state energies in the $\langle S_{\text{tot}}^z \rangle = 2, 1, 0, -1, \text{ and } -2$ sectors are degenerate. Note that even though the edge magnetization stands, the edge state in the spin-2 Haldane phase is not protected by any symmetry as the nondegenerate entanglement spectrum indicates [24, 25, 29]. With these discussions, we identify the phase II as the spin-2 Haldane phase.

IV. PERTURBATION THEORY

In this section, we identify the $c = 1$ CFT in the phase I. For this purpose, we split the Hamiltonian (1) into two parts:

$$\mathcal{H} = \mathcal{H}_0 + V, \quad (9)$$

where \mathcal{H}_r and V are the intra-tetrahedron and inter-tetrahedron interactions, respectively:

$$\mathcal{H}_0 = \sum_r h_r, \quad (10a)$$

$$h_r = J(\mathbf{S}_{r,1} \cdot \mathbf{S}_{r,2} + \mathbf{S}_{r,2} \cdot \mathbf{S}_{r,3} + \mathbf{S}_{r,3} \cdot \mathbf{S}_{r,1}) + \alpha J \mathbf{S}_{r,4} \cdot \mathbf{T}_r, \quad (10b)$$

and

$$V = J_t \sum_{r=1}^L \mathbf{S}_{r,4} \cdot \mathbf{T}_{r+1} + J_\ell \sum_{r=1}^L \sum_{n=1}^3 \mathbf{S}_{r,n} \cdot \mathbf{S}_{r+1,n}. \quad (11)$$

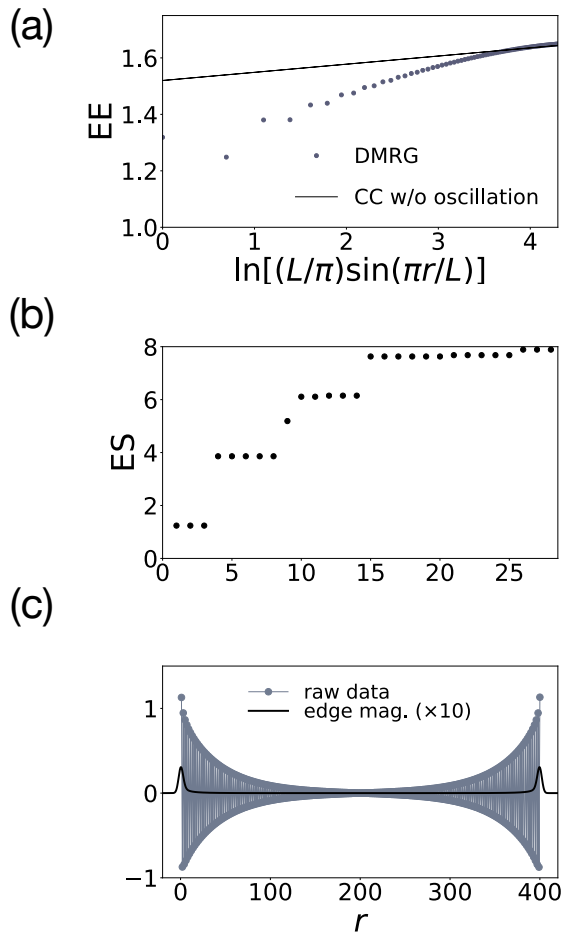


FIG. 4. (a) Entanglement entropy in phase II. (b) Entanglement spectrum in phase II. (c) Edge magnetizations in phase II. In the three panels, filled balls are DMRG data with $L = 400$, $J_t/J = 0.2$, $J_\ell = 0.1$, and $\alpha = -3.5$. The DMRG calculations are done with $\langle S_{\text{tot}}^z \rangle = 2$ to minimize the boundary effects. The solid curve is the Calabrese-Cardy formula (2) without the boundary term ($b = 0$). The entanglement entropy does not fit well with the Calabrese-Cardy formula, implying that the phase II is gapped. The entanglement spectrum shows no special degeneracy in contrast to the phase I, implying that the phase II is topologically trivial. The edge magnetization implies that the phase II is the spin-2 Haldane one because of the quantized edge magnetizations, $(M_{\text{left}}^z, M_{\text{right}}^z) = (0.99999, 1.00001)$.

We regard V as a perturbation to \mathcal{H}_0 . In other words, we regard J_t/J and J_ℓ/J small perturbative parameters.

A. Unperturbed ground states

The unperturbed Hamiltonian (10a) describes mutually isolated tetrahedra. Each tetrahedron is governed

by the simple Hamiltonian (10b) paraphrased as

$$h_r = \frac{J(1-\alpha)}{2} \mathbf{T}_r^2 + \frac{\alpha J}{2} \mathbf{S}_{r,\text{tot}}^2 + \text{const.} \quad (12)$$

This Hamiltonian consists only of \mathbf{T}_r of the base triangle and the total spin $\mathbf{S}_{r,\text{tot}} = \mathbf{T}_r + \mathbf{S}_{r,4} = \sum_{n=1}^4 \mathbf{S}_{r,n}$ of the tetrahedron. The Hamiltonian (12) conserves the spin quantum numbers $T_r = 1/2$ or $3/2$ of \mathbf{T}_r and $S_{r,\text{tot}} = 0, 1$, or 2 of $\mathbf{S}_{r,\text{tot}}$, and the z component $S_{r,\text{tot}}^z$ of $\mathbf{S}_{r,\text{tot}}$. Every eigenstate is thus labeled by at least three parameters, which we denote $|T_r, S_{r,\text{tot}}, S_{r,\text{tot}}^z\rangle$.

We can easily find a ground state of the Hamiltonian (12) by solving the eigenvalue equation. For $\alpha < -3$, the ground state of h_r has $T_r = 3/2$ and $S_{r,\text{tot}} = 2$, where the ground state is five-fold degenerate: $|\frac{3}{2}, 2, m\rangle$ with $m = 2, 1, 0, -1, -2$. For $-3 < \alpha < 0$, the ground state has $T_r = 1/2$ and $S_{r,\text{tot}} = 1$, but is six-fold degenerate: $|\frac{1}{2}, 1, m, \chi\rangle$ with $m = 1, 0, -1$ and $\chi = \pm 1$. Here, the ground state admits the additional parameter $\chi = \pm 1$ that represents the eigenvalue of a scalar chirality,

$$\chi_r = \frac{4}{3\sqrt{3}} (\mathbf{S}_{r,1} \cdot \mathbf{S}_{r,2} \times \mathbf{S}_{r,3} + \mathbf{S}_{r,2} \cdot \mathbf{S}_{r,3} \times \mathbf{S}_{r,1} + \mathbf{S}_{r,3} \cdot \mathbf{S}_{r,1} \times \mathbf{S}_{r,2}). \quad (13)$$

This scalar chirality is defined on the base triangle of the tetrahedron but can also be identified as the chirality of the tetrahedron since $\alpha \neq 1$ [Fig. 1 (b)]. The chirality (13) is a central figure in this paper. We determined the factor $4/3\sqrt{3}$ from explicit representations of the eigenstates.

Generally, chirality degrees of freedom affect magnetism when the magnetic configuration is canted and noncollinear [30]. The geometrical frustration can trigger such magnetic configurations with nonzero scalar chirality. In our tetrahedron, the chirality must be incorporated for $-3 < \alpha < 0$, where the geometrically frustrated interaction $J(\mathbf{S}_{r,1} \cdot \mathbf{S}_{r,2} + \mathbf{S}_{r,2} \cdot \mathbf{S}_{r,3} + \mathbf{S}_{r,3} \cdot \mathbf{S}_{r,1})$ in the base triangle leads to a canted state with $T_r^z = \pm 1/2$. Let us denote the eigenstate of the base triangle as $|T_r^z, \chi\rangle_{123}$. For $T_r^z = 1/2$, they are given by

$$|\frac{1}{2}, +\rangle_{123} = \frac{1}{\sqrt{3}} (|\downarrow_1 \uparrow_2 \uparrow_3\rangle + \omega |\uparrow_1 \downarrow_2 \uparrow_3\rangle + \omega^{-1} |\uparrow_1 \uparrow_2 \downarrow_3\rangle), \quad (14)$$

$$|\frac{1}{2}, -\rangle_{123} = \frac{1}{\sqrt{3}} (|\downarrow_1 \uparrow_2 \uparrow_3\rangle + \omega^{-1} |\uparrow_1 \downarrow_2 \uparrow_3\rangle + \omega |\uparrow_1 \uparrow_2 \downarrow_3\rangle), \quad (15)$$

with a complex constant $\omega = \exp(i\frac{2\pi}{3})$ and an eigenstate $|s_1 s_2 s_3\rangle$ with $S_{r,n}^z = s_n$ for $n = 1, 2, 3$. It is easy to verify that these $|\frac{1}{2}, \chi\rangle_{123}$ satisfy

$$\chi_r |\frac{1}{2}, \chi\rangle_{123} = \chi |\frac{1}{2}, \chi\rangle_{123}. \quad (16)$$

We can build the eigenstate $|\frac{1}{2}, 1, m, \chi\rangle$ by combining $|\pm\frac{1}{2}, \chi\rangle_{123}$ and eigenstates $|\uparrow\rangle_4$ and $|\downarrow\rangle_4$ of $S_{r,4}^z$ ferromagnetically [Eq. (A1)].

The ground state of h_r switches at $\alpha = -3$, a close value to the transition point $\alpha_c \approx -2.7$ obtained from Fig. 1 (c). We may regard $\alpha_c = -3$ as the zeroth-order perturbation value of the phase transition point with respect to J_t/J and J_ℓ/J .

B. Degenerate perturbation theory in phase I

We focus ourselves on the phase I in the range $\alpha_c < \alpha < 0$ and take the J_t and J_ℓ interactions into account. These interactions lift the degeneracy of the unperturbed ground state. To describe the perturbation theory, we prepare an effective $S = 1$ spin \mathbf{s}_r and an effective $S = 1/2$ pseudospin \mathbf{t}_r from the sixfold degenerate ground states $|\frac{1}{2}, 1, m, \chi\rangle$ of h_r . The z components of these spins are defined as

$$s_r^z |\frac{1}{2}, 1, m, \chi\rangle = m |\frac{1}{2}, 1, m, \chi\rangle, \quad (17)$$

$$t_r^z |\frac{1}{2}, 1, m, \chi\rangle = \frac{\chi}{2} |\frac{1}{2}, 1, m, \chi\rangle. \quad (18)$$

The raising operators s_r^+ and t_r^+ increase the z components m and $\chi/2$ by 1, respectively. The lowering operators are defined similarly. We can derive a low-energy effective representation of the spin operator $\mathbf{S}_{r,n}$ by projecting the operator into the low-energy Hilbert subspace (see Appendix. B):

$$\mathbf{S}_{r,n} \sim \frac{1}{6}(1 - 2\omega^{n-1}t_r^+ - 2\omega^{-(n-1)}t_r^-) \otimes \mathbf{s}_r, \quad (19)$$

$$\mathbf{S}_{r,4} \sim \frac{1}{2}\mathbf{s}_r, \quad (20)$$

for $n = 1, 2, 3$. Here, the symbol \sim means an approximate identity in the low-energy Hilbert subspace well below the spin gap.

The low-energy physics of the tetrahedral spin chain (1) is effectively described by \mathbf{s}_r and \mathbf{t}_r . The perturbation expansion with respect to J_t and J_ℓ leads to the low-energy effective Hamiltonian:

$$\begin{aligned} \mathcal{H}_{\text{eff}} \approx & \frac{3J_t + J_\ell}{12} \sum_{r=1}^L \mathbf{s}_r \cdot \mathbf{s}_{r+1} \\ & + \frac{J_\ell}{12} \sum_{r=1}^L (t_r^x t_{r+1}^x + t_r^y t_{r+1}^y) \mathbf{s}_r \cdot \mathbf{s}_{r+1}, \end{aligned} \quad (21)$$

where the second- and higher-order terms are discarded. Within the first-order approximation, we obtain the effective Hamiltonian (21) by replacing the four spins $\mathbf{S}_{r,n}$ ($n = 1, 2, 3, 4$) with their effective low-energy representations, Eqs. (19) and (20).

We can confirm that the right hand side of the Hamiltonian (21) indeed has the gSPT ground state. The first line of Eq. (21) is the spin-1 Heisenberg antiferromagnetic interaction that trivially opens the spin gap. When J_t is larger than J_ℓ , the second line of Eq. (21) does not

close the spin gap. Note that the trivial spin-gap opening keeps the lattice translation symmetry. The lattice translation symmetry makes the ground-state expectation value $\langle \mathbf{s}_r \cdot \mathbf{s}_{r+1} \rangle = C_1$ spatially uniform. In other words, the constant C_1 is independent of the unit-cell index r . Then, we may further approximate Eq. (21) as

$$\begin{aligned} \mathcal{H}_{\text{eff}} \approx & \frac{3J_t + J_\ell}{12} \sum_{r=1}^L \mathbf{s}_r \cdot \mathbf{s}_{r+1} \\ & + \frac{C_1 J_\ell}{12} \sum_{r=1}^L (t_r^x t_{r+1}^x + t_r^y t_{r+1}^y), \end{aligned} \quad (22)$$

where the spin-1 \mathbf{s}_r and the spin-1/2 \mathbf{t}_r are effectively decoupled. The approximation (22) holds when we are concerned with the ground state and low-energy excitations well below the spin gap. To know the precise value of C_1 , we need a self-consistent determination process to include the effects of the pseudospin \mathbf{t}_r . However, the precise value is not important. Irrespective of sign of $C_1 J_\ell$, the second line of (22) represents that the pseudospin \mathbf{t}_r forms the TLL ground state. This TLL is known as the chirality liquid [31].

Since the $S = 1/2$ pseudospin \mathbf{t}_r follows the XY chain in Eq. (22), we can bosonize the pseudospin as

$$t_r^z = \frac{1}{\pi} \partial_x \phi + a_1 \sin(2\phi), \quad (23)$$

$$t_r^\pm = e^{i\theta} [(-1)^r b_0 + b_1 \sin(2\phi)], \quad (24)$$

where a_1 , b_0 , and b_1 are constants, $\phi(r)$ is a U(1) compact boson field, and $\theta(r)$ is its canonical conjugate that satisfy a commutation relation $[\phi(x), \theta(y)] = \pi i \Theta(x - y)$. Here, $\Theta(z)$ is the Heaviside step function with $\Theta(0) = 1/2$. We can bosonize the XY interaction of the pseudospin similarly to that of the authentic spin [19]:

$$\mathcal{H}_{\text{eff}} \approx \frac{v}{2\pi} \int dr \{ (\partial_r \theta)^2 + (\partial_r \phi)^2 \}, \quad (25)$$

where we dropped the \mathbf{s}_r part because it only generates high-energy excitations. The Hamiltonian (25) describes the $c = 1$ CFT of the free boson ϕ [32]. We thus identify the ground state of the phase I as the chirality liquid with symmetry-protected edge spins.

However, our argument thus far is only half the battle. The effective Hamiltonian (21) and its final form (25) hold only within the first-order approximation of J_t/J and J_ℓ/J . Higher-order terms of the perturbation expansion yield various interactions. To conclude that the phase I is the gSPT phase, we need to confirm that the higher-order corrections to the effective Hamiltonian (21) do not trivially open the gap. For example, if the effective Hamiltonian should admit an interaction $\sum_r t_r^x \propto \int dr \cos \theta$, the chirality liquid would immediately acquire the excitation gap and make the ground state unique and gapped. Fortunately, we have a complete list of the relevant interactions in the sense of the renormalization group: $\cos(p\theta)$, $\sin(p\theta)$ for $p = 1, 2$,

$\cos(2\phi)$, $\sin(2\phi)$, $\partial_x\phi$, and $\partial_x\theta$. Carefully analyzing what symmetry forbids these relevant interactions, we can discuss the ingappability of the chirality liquid. Reference [31] adopts this strategy to discuss the ingappability of the chirality liquid of an $S = 1/2$ three-leg spin tube on a $1/3$ magnetization plateau. In the next section, we adopt a more generic approach to show the ingappability and later come back to the specific case of the chirality liquid.

V. LSM THEOREM FOR DISCRETE SYMMETRIES

In this section, we show the ingappability of the phase I under symmetries from the viewpoint of the Lieb-Schultz-Mattis (LSM) theorem for discrete symmetries. The LSM theorem is a well-known no-go theorem about the ingappability of quantum phases [33–36]. As a fundamental principle that determines the fate of the quantum phase, the LSM theorem has long been discussed and applied to a wide variety of many-body systems [14, 34–45]. The LSM theorem and ingappability are essential to characterize the gSPT phase [13].

We give our attention to a \mathbb{Z}_3 symmetry, a \mathbb{Z}_2^T symmetry, and the lattice translation symmetry ($\mathbf{S}_{r,n} \rightarrow \mathbf{S}_{r+1,n}$). Here, \mathbb{Z}_3 represents the \mathbb{Z}_3 rotation symmetry around an axis piercing spins $\mathbf{S}_{r,4}$ for $r = 1, 2, \dots, L$ [the dashed blue line of Fig. 1 (b)].

$$\mathcal{R}\mathbf{S}_{r,n}\mathcal{R}^{-1} = \mathbf{S}_{r,n'}, \quad (26)$$

with

$$n' = \begin{cases} 2, & (n = 1), \\ 3, & (n = 2), \\ 1, & (n = 3), \\ 4, & (n = 4). \end{cases} \quad (27)$$

\mathbb{Z}_2^T represents the time-reversal symmetry,

$$\mathcal{T}\mathbf{S}_{r,n}\mathcal{T}^{-1} = -\mathbf{S}_{r,n}, \quad (28a)$$

$$\mathcal{T}i\mathcal{T}^{-1} = -i. \quad (28b)$$

Our argument is basically a derivative of a method used in Ref. [46] to show a LSM theorem for discrete symmetries.

A. Gauging global \mathbb{Z}_3 symmetry

The LSM theorem is closely related to an 't Hooft anomaly [14, 15]. The 't Hooft anomaly is an inconsistency between plural global symmetries that appears when gauging one of the global symmetries, i.e., when promoting the symmetry to a local gauge symmetry [47, 48]. In the presence of the local gauge symmetry, the excitation spectrum is invariant under a local

gauge transformation. The local gauge transformation is also referred to as a local gauge twist [49–53]. The local gauge symmetry motivates us to consider a closed boundary condition accompanied by a local gauge twist on its seam instead of the PBC. Let us call this boundary condition a symmetry-twisted boundary condition (STBC) following Ref. [46]. If we gauge the global \mathbb{Z}_3 symmetry, the corresponding STBC, which we call a \mathbb{Z}_3 STBC, is defined as

$$\mathbf{S}_{r+L,n} = \mathbf{S}_{r,n'}, \quad (29)$$

with n' of Eq. (27). Only when we pass over the seam of the system, we locally feel the \mathbb{Z}_3 spatial rotation.

The Hamiltonian with the \mathbb{Z}_3 STBC is

$$\begin{aligned} \mathcal{H}_R = & J \sum_{r=1}^L (\mathbf{S}_{r,1} \cdot \mathbf{S}_{r,2} + \mathbf{S}_{r,2} \cdot \mathbf{S}_{r,3} + \mathbf{S}_{r,3} \cdot \mathbf{S}_{r,1}) \\ & + \alpha J \sum_{r=1}^L \mathbf{S}_{r,4} \cdot \mathbf{T}_r \\ & + J_t \sum_{r=1}^L \mathbf{S}_{r,4} \cdot \mathbf{T}_{r+1} + J_\ell \sum_{r=1}^{L-1} \sum_{n=1}^3 \mathbf{S}_{r,n} \cdot \mathbf{S}_{r+1,n} \\ & + J_\ell (\mathbf{S}_{L,1} \cdot \mathbf{S}_{1,2} + \mathbf{S}_{L,2} \cdot \mathbf{S}_{1,3} + \mathbf{S}_{L,3} \cdot \mathbf{S}_{1,1}). \end{aligned} \quad (30)$$

The last interaction on the seam of the \mathbb{Z}_3 STBC gets twisted (rotated) by the local \mathbb{Z}_3 gauge transformation. With the \mathbb{Z}_3 STBC, the lattice translation \tilde{T}_1 is given by

$$\tilde{T}_1 \mathbf{S}_{j,n} \tilde{T}_1^{-1} = \begin{cases} \mathbf{S}_{j+1,n}, & (j \neq L), \\ \mathbf{S}_{1,n'}, & (j = L), \end{cases} \quad (31)$$

with n' of Eq. (27). This lattice translation operator admits a simple representation,

$$\tilde{T}_1 = R_1 T_1 = T_1 R_L. \quad (32)$$

Here, T_1 is the lattice translation in the PBC and R_j is the \mathbb{Z}_3 rotation that locally acts on the j th tetrahedron, that is,

$$T_1 \mathbf{S}_{j,n} T_1^{-1} = \mathbf{S}_{j+1,n}, \quad (33)$$

$$R_j \mathbf{S}_{k,n} R_j^{-1} = \delta_{j,k} \mathbf{S}_{j,n'} + (1 - \delta_{j,k}) \mathbf{S}_{j,n}. \quad (34)$$

The global \mathbb{Z}_3 symmetry is generated by $\mathcal{R} = R_1 R_2 \cdots R_L$. The lattice translation (32) is a straightforward generalization of that of Ref. [46]. We can confirm that $[\tilde{T}_1, \mathcal{H}_R] = 0$ and $[T_1, \mathcal{H}_R] \neq 0$. In addition, the Hamiltonian (30) has the time-reversal symmetry, $[\mathcal{T}, \mathcal{H}_R] = 0$. It is noteworthy that the \mathbb{Z}_3 rotation and the time-reversal symmetries are commutative,

$$[\mathcal{T}, \mathcal{R}] = 0. \quad (35)$$

B. Ingappability

With these preparations, we show by contradiction the ingappability of the phase I under the $\mathbb{Z}_3 \times \mathbb{Z}_2^T$ and the

lattice translation symmetries. A key observation is that the unique gapped ground state is insensitive to the local gauge twist. That is, when the ground state of the Hamiltonian (1) with the PBC is unique and gapped, so is the ground state of the Hamiltonian (30) with the STBC. This insensitivity of the ground state to the local gauge twist is not rigorously proven but a physically sound conjecture [46, 54]. Hence, to show the anomaly between the $\mathbb{Z}_3 \times \mathbb{Z}_2^T$ symmetry and the translation symmetry, it suffices to find a contradiction by assuming the unique gapped ground state under the STBC.

Let $|\psi_0\rangle_R$ be the unique gapped ground state of the Hamiltonian with the STBC (30). We represent the ground state as

$$|\psi_0\rangle_R = \sum_{i_1, i_2, \dots, i_L} c_{i_1 i_2 \dots i_L} |i_1 i_2 \dots i_L\rangle, \quad (36)$$

with $c_{i_1 i_2 \dots i_L} \in \mathbb{C}$ and a product state $|i_1 i_2 \dots i_L\rangle = |i_1\rangle \otimes |i_2\rangle \otimes \dots \otimes |i_L\rangle$ with $i_r = 1, 2, \dots, 6$ for all $r = 1, 2, \dots, L$. We use a basis,

$$|\frac{1}{2}, 1, 1, +\rangle = |1\rangle, \quad (37a)$$

$$|\frac{1}{2}, 1, 0, +\rangle = |2\rangle, \quad (37b)$$

$$|\frac{1}{2}, 1, -1, +\rangle = |3\rangle, \quad (37c)$$

$$|\frac{1}{2}, 1, 1, -\rangle = |4\rangle, \quad (37d)$$

$$|\frac{1}{2}, 1, 0, -\rangle = |5\rangle, \quad (37e)$$

$$|\frac{1}{2}, 1, -1, -\rangle = |6\rangle. \quad (37f)$$

We can take the ground state (36) as an eigenstate of \tilde{T}_1 :

$$\tilde{T}_1 |\psi_0\rangle_R = e^{iP_0} |\psi_0\rangle \quad (38)$$

with $P_0 \in [0, 2\pi)$.

Now we consider a state

$$|\psi'_0\rangle_R = \mathcal{T} |\psi_0\rangle_R. \quad (39)$$

If $|\psi_0\rangle_R$ was the unique gapped ground state, $|\psi'_0\rangle_R$ would be identical to $|\psi_0\rangle_R$ except for a U(1) factor since $[\mathcal{H}_R, \mathcal{T}] = 0$. In what follows, we show that $|\psi'_0\rangle_R$ cannot be identical to $|\psi_0\rangle_R$ by looking into a \tilde{T}_1 eigenvalue of $|\psi'_0\rangle_R$:

$$\tilde{T}_1 |\psi'_0\rangle_R = e^{iP'_0} |\psi'_0\rangle_R. \quad (40)$$

It suffices to show $P'_0 \neq P_0 \pmod{2\pi}$. To calculate the left hand side of Eq. (40), we need to know how the time-reversal \mathcal{T} and the local \mathbb{Z}_3 spatial rotation R_r act on $|i_r\rangle$. They act on $|i_r\rangle$ as [Eqs. (B12) and (B13)]

$$\mathcal{T} |i_r\rangle = \sum_{j_r=1}^6 \left(-2t_r^x \otimes \exp(i\pi s_r^z) \right)_{i_r j_r} |j_r\rangle, \quad (41)$$

$$R_r |i_r\rangle = \sum_{j_r=1}^6 \left(\exp\left(i\frac{4\pi}{3} t_r^z\right) \otimes \mathbb{1}_3 \right)_{i_r j_r} |j_r\rangle. \quad (42)$$

The time reversal \mathcal{T} turns into the π rotations:

$$\mathcal{T}(s_r^x, s_r^y, s_r^z) \mathcal{T}^{-1} \sim (s_r^x, -s_r^y, -s_r^z), \quad (43a)$$

$$\mathcal{T}(t_r^x, t_r^y, t_r^z) \mathcal{T}^{-1} \sim (t_r^x, -t_r^y, -t_r^z). \quad (43b)$$

The global \mathbb{Z}_3 spatial rotation $\mathcal{R} = R_1 R_2 \dots R_L$ acts only on the pseudospin:

$$\mathcal{R} t_r^z \mathcal{R}^{-1} \sim t_r^z, \quad (44a)$$

$$\mathcal{R} t_r^\pm \mathcal{R}^{-1} \sim \omega t_r^\pm. \quad (44b)$$

The symmetry operations (41) and (42) lead to

$$R_r \mathcal{T} |i_r\rangle = \mathcal{T} R_r^{-1} |i_r\rangle. \quad (45)$$

The relation (45) comes from the anticommutation relation

$$t_j^x t_j^z = -t_j^z t_j^x, \quad (46)$$

of the spin-1/2 operator \mathbf{t}_j . The left hand side of Eq. (40) thus becomes

$$\tilde{T}_1 |\psi'_0\rangle_R = e^{iP_0} R_1^{-1} |\psi'_0\rangle_R. \quad (47)$$

Equations (40) and (47) lead to

$$R_1 |\psi'_0\rangle_R = e^{i(P_0 - P'_0)} |\psi'_0\rangle_R. \quad (48)$$

That is, $|\psi'_0\rangle_R$ is an eigenstate of the local \mathbb{Z}_3 rotation operator R_1 . Since R_1 has the eigenvalue $\exp(\pm \frac{2\pi i}{3})$ [Eq. (42)], we obtain

$$P'_0 = P_0 \pm \frac{2\pi}{3} \pmod{2\pi}. \quad (49)$$

Hence, $|\psi'_0\rangle_R$ and $|\psi_0\rangle_R$ are the doubly degenerate ground states that spontaneously breaks the time-reversal symmetry, which contradicts the assumption of the unique gapped ground state. Therefore, we conclude the anomaly between $\mathbb{Z}_3 \times \mathbb{Z}_2^T$ symmetry and the lattice translation symmetry. In other words, the tetrahedral chain (1) cannot have the unique gapped ground state in the presence of the $\mathbb{Z}_3 \times \mathbb{Z}_2^T$ and the lattice translation symmetries as long as the chirality degrees of freedom govern the low-energy physics.

Our argument about the anomaly relies only on symmetries of the $S = 1$ spin \mathbf{s}_r and the $S = 1/2$ pseudospin \mathbf{t}_r . However, there is a precondition that the low-energy Hilbert subspace is locally spanned by the six states (37), where we implicitly assume the U(1) spin-rotation symmetry around S^z . Should the U(1) spin-rotation symmetry be absent, those low-energy states would be mixed with other local eigenstates with $S_{r,\text{tot}} \neq 1$ and would violate the above precondition. Therefore, we need the $\mathbb{Z}_3 \times \mathbb{Z}_2^T$, lattice translation, and U(1) spin-rotation symmetries to make the gSPT phase ingappable.

C. Discussions

1. Applicability

Our argument in the previous subsections generically holds when the unit cell contains the six local low-energy state $|i_r\rangle$ (37) irrespective of how neighboring tetrahedra are coupled. Hence, the ingappability holds even when we replace the interaction (11) with a completely different interaction unless it violates one of the \mathbb{Z}_3 , the \mathbb{Z}_2^T , the lattice translation, and the U(1) spin-rotation symmetries.

2. Specific case: chirality liquid

However, since we are concerned with the chirality liquid, we should go back to this specific case and translate the generic result into the language of the chirality liquid (25).

Let us check that the relevant interactions, $\cos(2\phi)$, $\sin(2\phi)$, $\cos(p\theta)$, $\sin(p\theta)$ for $p = 1, 2$, $\partial_x\phi$, and $\partial_x\theta$, of the $c = 1$ CFT (25) are all forbidden by the above-mentioned symmetries. The action of the \mathbb{Z}_3 symmetry is simple. The global \mathbb{Z}_3 rotation affects only the pseudospin [Eq. (44)]. In terms of the boson fields (23) and (24), they read as

$$\mathcal{R}\phi(r)\mathcal{R}^{-1} = \phi(r), \quad (50)$$

$$\mathcal{R}\theta(r)\mathcal{R}^{-1} = \theta(r) + \frac{2\pi}{3}. \quad (51)$$

The \mathbb{Z}_3 symmetry thus forbids $\cos(p\theta)$ and $\sin(p\theta)$ for $p = 1, 2$.

The lattice translation acts on

$$T_1 \mathbf{s}_r T_1^{-1} = \mathbf{s}_{r+1}, \quad (52)$$

$$T_1 \mathbf{t}_r T_1^{-1} = \mathbf{t}_{r+1}. \quad (53)$$

Note that we imposed the PBC on the tetrahedral chain. The latter reads as

$$T_1 \phi(r) T_1^{-1} = \phi(r) + \frac{\pi}{2}, \quad (54)$$

$$T_1 \theta(r) T_1^{-1} = \theta(r) + \pi. \quad (55)$$

The lattice translation thus forbids $\cos(2\phi)$, $\sin(2\phi)$, $\cos\theta$, and $\sin\theta$. Imposing the \mathbb{Z}_3 rotation and the lattice translation symmetries, we can forbid the relevant interactions except for $\partial_x\phi$ and $\partial_x\theta$.

Let us show that the time-reversal symmetry forbids them. In the chirality-liquid phase I, the time-reversal (41) works as the π rotations around the x axis at low energies [Eq. (43)]. $t_r^x = (t_r^+ + (t_r^+)^\dagger)/2$ and $t_r^y = (t_r^+ - (t_r^+)^\dagger)/2$ are written as

$$t_r^x = (-1)^r b_0 \cos\theta + i b_1 \sin\theta \sin(2\phi), \quad (56)$$

$$t_r^y = (-1)^r b_0 \sin\theta - i b_1 \cos\theta \sin(2\phi), \quad (57)$$

because of $[\phi(x), \theta(x)] = i\pi/2$. These bosonization formulas lead us to the following action of the time reversal \mathcal{T} :

$$\mathcal{T}\phi(r)\mathcal{T}^{-1} = -\phi(r), \quad (58)$$

$$\mathcal{T}\theta(r)\mathcal{T}^{-1} = -\theta(r). \quad (59)$$

The \mathbb{Z}_2^T symmetry thus forbids $\partial_x\phi$ and $\partial_x\theta$. These interactions do not immediately open the gap but eventually does [55]. In fact, adding an interaction

$$g \sum_{r=1}^L \chi_r \approx 2g \sum_{r=1}^L t_r^z \approx \frac{2g}{\pi} \int_0^L dr \partial_r \phi, \quad (60)$$

to the Hamiltonian (21) or (25) eventually opens the pseudospin gap by driving the chirality-liquid ground state to the spin-1 Haldane state.

VI. SUMMARY

We discussed the gSPT phase of the geometrically frustrated tetrahedral spin chain (1) [Figs. 1 (a) and (b)]. The unit cell contains one tetrahedron with four localized spins. Within each tetrahedron, three bonds are antiferromagnetic ($J > 0$) and the other three bonds are ferromagnetic ($\alpha J < 0$). For $\alpha_c < \alpha < 0$ with $\alpha_c \approx -0.27$, the ground state of this tetrahedral spin chain belongs to the gSPT phase [the phase I of Fig. 1 (c)].

We amassed the numerical evidences that the phase I indeed qualifies as the gSPT phase (Sec. III). With the finite-size DMRG calculations under the OBC, we confirmed that the phase I is described by the $c = 1$ CFT (Fig. 2) and at the same time, accompanied by the $S = 1/2$ edge spin on each end of the spin chain (Fig. 3).

To get insight into the phase I, we further developed the degenerate perturbation theory (Sec. IV). The perturbation theory uncovered that the $c = 1$ CFT is the TLL of the chirality liquid [31]. The spin and chirality degrees of freedom are strongly coupled with each other at the Hamiltonian level (21). Since the tetrahedral spin chain with four spins per unit cell can trivially open the spin gap, the low-energy physics is fully written in terms of the chirality.

In the last section V, we showed the ingappability of the chirality liquid under the $\mathbb{Z}_3 \times \mathbb{Z}_2^T$ symmetry, the lattice translation symmetry, and the U(1) spin-rotation symmetry, where \mathbb{Z}_3 and \mathbb{Z}_2^T refer to the \mathbb{Z}_3 spatial rotation around the legs and the time reversal, respectively. Here, we showed the ingappability by extending the argument of Ref. [46] based on the STBC. This argument clarified the existence of the 't Hooft anomaly of the lattice system without mapping it to a quantum field theory. The anomaly (or equivalently, the ingappability) is directly related to the stability of the gSPT phase. Should the anomaly be absent, the ground state in the gSPT phase would easily acquire the excitation gap without spontaneously breaking any symmetry. In our gSPT

phase of the chirality liquid with $S = 1/2$ edge spins, the $S = 1/2$ edge states is protected by the same symmetry as that protects the spin-1 Haldane phase, namely, at least one of the $D_2 \cong \mathbb{Z}_2 \times \mathbb{Z}_2$ spin-rotation symmetry, the time-reversal symmetry, and the bond-centered inversion symmetry.

ACKNOWLEDGMENTS

The authors are grateful to Shigetoshi Sota, Yasuhiro Tada, and Hiroshi Ueda for fruitful discussions. This work was supported by JSPS Grants-in-Aid for Transformative Research Areas (A) ‘‘Extreme Universe’’ Nos. JP21H05191 and 21H05182 (S.C.F.) and JSPS KAKENHI Grant Nos. JP20K03769 and 21K03465 (S.C.F.).

Appendix A: Unperturbed ground states

We write down the unperturbed ground state $|\frac{1}{2}, 1, m, \chi\rangle$ of h_r in terms of $|T_r^z, \chi\rangle_{123} |m\rangle_4$, where $|T_r^z, \chi\rangle_{123}$ is the eigenstate of the z component T_r^z of \mathbf{T}_r and the chirality $\chi = \pm 1$ and $|m\rangle_4$ is the eigenstate of $S_{r,\text{tot}}^z = m$. Since \mathbf{T}_r and $\mathbf{S}_{r,4}$ are ferromagnetically coupled to form the $S = 1$ spin, the unperturbed ground state $|\frac{1}{2}, 1, m, \chi\rangle$ are written as

$$|\frac{1}{2}, 1, 1, \chi\rangle = |\frac{1}{2}, \chi\rangle_{123} |\frac{1}{2}\rangle_4, \quad (\text{A1a})$$

$$|\frac{1}{2}, 1, 0, \chi\rangle = \frac{1}{\sqrt{2}}(|\frac{1}{2}, \chi\rangle_{123} |-\frac{1}{2}\rangle_4 + |-\frac{1}{2}, \chi\rangle_{123} |\frac{1}{2}\rangle_4), \quad (\text{A1b})$$

$$|\frac{1}{2}, 1, -1, \chi\rangle = |-\frac{1}{2}, \chi\rangle_{123} |-\frac{1}{2}\rangle_4. \quad (\text{A1c})$$

It is helpful to look into contents of $|\pm\frac{1}{2}, \chi\rangle_{123}$. Let $|m_1 m_2 m_3\rangle$ be an eigenstate of $S_{r,n}^z = m_n$ for $n = 1, 2, 3$. We represent the eigenvalue $m_n = 1/2$ and $-1/2$ as $m_n = \uparrow$ and \downarrow , respectively. For example, $|\uparrow_1 \uparrow_2 \downarrow_3\rangle$ be an eigenstate of $S_{r,n}^z$ for $n = 1, 2, 3$ with eigenvalues $S_{r,1}^z = S_{r,2}^z = 1/2$ and $S_{r,3}^z = -1/2$. We can write $|\pm\frac{1}{2}, \chi\rangle_{123}$ as

$$|\frac{1}{2}, +\rangle_{123} = \frac{1}{\sqrt{3}}(|\downarrow_1 \uparrow_2 \uparrow_3\rangle + \omega |\uparrow_1 \downarrow_2 \uparrow_3\rangle + \omega^{-1} |\uparrow_1 \uparrow_2 \downarrow_3\rangle), \quad (\text{A2a})$$

$$|\frac{1}{2}, -\rangle_{123} = \frac{1}{\sqrt{3}}(|\downarrow_1 \uparrow_2 \uparrow_3\rangle + \omega^{-1} |\uparrow_1 \downarrow_2 \uparrow_3\rangle + \omega |\uparrow_1 \uparrow_2 \downarrow_3\rangle), \quad (\text{A2b})$$

$$|-\frac{1}{2}, +\rangle_{123} = \frac{1}{\sqrt{3}}(|\uparrow_1 \downarrow_2 \downarrow_3\rangle + \omega |\downarrow_1 \uparrow_2 \downarrow_3\rangle + \omega^{-1} |\downarrow_1 \downarrow_2 \uparrow_3\rangle), \quad (\text{A2c})$$

$$|-\frac{1}{2}, -\rangle_{123} = \frac{1}{\sqrt{3}}(|\uparrow_1 \downarrow_2 \downarrow_3\rangle + \omega^{-1} |\downarrow_1 \uparrow_2 \downarrow_3\rangle + \omega |\downarrow_1 \downarrow_2 \uparrow_3\rangle), \quad (\text{A2d})$$

with $\omega = \exp(2\pi i/3)$. These eigenstates satisfy

$$\chi_r^z |\pm\frac{1}{2}, \chi\rangle = \chi |\pm\frac{1}{2}, \chi\rangle, \quad (\text{A3})$$

where χ_r is a scalar chirality of the base triangle (13).

Appendix B: Pseudospin representation

Here, we show technical details of the pseudospin representation of $\mathbf{S}_{r,n}$. Let us denote the projection operator onto the unperturbed ground state of h_r as P_r . We can explicitly write P_r as

$$P_r = \sum_{m=1,0,-1} \sum_{\chi=\pm} |\frac{1}{2}, 1, m, \chi\rangle \langle \frac{1}{2}, 1, m, \chi|. \quad (\text{B1})$$

We adopt a basis to represent $|\frac{1}{2}, 1, m, \chi\rangle$ as

$$|\frac{1}{2}, 1, 1, +\rangle = |1\rangle = (1, 0, 0, 0, 0, 0)^\top, \quad (\text{B2a})$$

$$|\frac{1}{2}, 1, 0, +\rangle = |2\rangle = (0, 1, 0, 0, 0, 0)^\top, \quad (\text{B2b})$$

$$|\frac{1}{2}, 1, -1, +\rangle = |3\rangle = (0, 0, 1, 0, 0, 0)^\top, \quad (\text{B2c})$$

$$|\frac{1}{2}, 1, 1, -\rangle = |4\rangle = (0, 0, 0, 1, 0, 0)^\top, \quad (\text{B2d})$$

$$|\frac{1}{2}, 1, 0, -\rangle = |5\rangle = (0, 0, 0, 0, 1, 0)^\top, \quad (\text{B2e})$$

$$|\frac{1}{2}, 1, -1, -\rangle = |6\rangle = (0, 0, 0, 0, 0, 1)^\top. \quad (\text{B2f})$$

With this basis, we can represent \mathbf{T}_r as

$$\begin{aligned} P_r T_r^z P_r &= P_r \begin{pmatrix} 1/2 & 0 & 0 & 0 & 0 & 0 \\ 0 & 0 & 0 & 0 & 0 & 0 \\ 0 & 0 & -1/2 & 0 & 0 & 0 \\ 0 & 0 & 0 & 1/2 & 0 & 0 \\ 0 & 0 & 0 & 0 & 0 & 0 \\ 0 & 0 & 0 & 0 & 0 & -1/2 \end{pmatrix} P_r \\ &= P_r \left(\frac{1}{2} \mathbb{1}_2 \otimes s_r^z \right) P_r, \end{aligned} \quad (\text{B3})$$

$$\begin{aligned} P_r T_r^+ P_r &= P_r \begin{pmatrix} 0 & -1/\sqrt{2} & 0 & 0 & 0 & 0 \\ 0 & 0 & -1/\sqrt{2} & 0 & 0 & 0 \\ 0 & 0 & 0 & 0 & 0 & 0 \\ 0 & 0 & 0 & 0 & -1/\sqrt{2} & 0 \\ 0 & 0 & 0 & 0 & 0 & -1/\sqrt{2} \\ 0 & 0 & 0 & 0 & 0 & 0 \end{pmatrix} P_r \\ &= P_r \left(-\frac{1}{2} \mathbb{1}_2 \otimes s_r^+ \right) P_r, \end{aligned} \quad (\text{B4})$$

$$P_r T_r^- P_r = P_r \left(-\frac{1}{2} \mathbb{1}_2 \otimes s_r^- \right) P_r, \quad (\text{B5})$$

where $\mathbb{1}_n$ denotes the $n \times n$ identity matrix. The total spin \mathbf{T}_r of the base triangle thus reads as the spin-1 operator $\frac{1}{2} \mathbf{s}_r$ at low energies. As expected, \mathbf{T}_r acts as the identity $\mathbb{1}_2$ on the chirality degrees of freedom. The minus sign on the right hand side of Eqs. (B4) and (B5) can be eliminated by a global symmetry operation transformation,

$$U_z := \exp \left(i\pi \sum_{r=1}^L \sum_{n=1}^4 S_{r,n}^z \right). \quad (\text{B6})$$

The application of U_z alters no results in this paper because we impose the U(1) spin-rotation symmetry around S^z on the system. U_z is included in this U(1) group. In what follows, we redefine $U_z \mathbf{S}_{r,n} U_z^{-1} = (-S_{r,n}^x, -S_{r,n}^y, S_{r,n}^z)$ as $\mathbf{S}_{r,n}$ for simplicity. This redefinition enables us to simplify the projection of \mathbf{T}_r :

$$P_r \mathbf{T}_r P_r = P_r \left(\frac{1}{2} \mathbb{1}_2 \otimes \mathbf{s}_r \right) P_r \quad (\text{B7})$$

Since two spin-1/2 $\mathbf{S}_{r,4}$ and \mathbf{T}_r form the spin-1 $\mathbf{S}_{r,\text{tot}}$, it immediately follows that

$$P_r \mathbf{S}_{r,4} P_r = P_r \mathbf{T}_r P_r = P_r \left(\frac{1}{2} \mathbb{1}_2 \otimes \mathbf{s}_r \right) P_r. \quad (\text{B8})$$

The other spins $\mathbf{S}_{r,n}$ ($n = 1, 2, 3$) nontrivially act on the chirality degrees of freedom. For example,

$$\begin{aligned} P_r S_{r,3}^z P_r &= P_r \begin{pmatrix} 1/6 & 0 & 0 & -\omega^{-1}/3 & 0 & 0 \\ 0 & 0 & 0 & 0 & 0 & 0 \\ 0 & 0 & -1/6 & 0 & 0 & \omega^{-1}/3 \\ -\omega/3 & 0 & 0 & 1/6 & 0 & 0 \\ 0 & 0 & 0 & 0 & 0 & 0 \\ 0 & 0 & \omega/3 & 0 & 0 & -1/6 \end{pmatrix} P_r \\ &= P_r \left(\frac{1}{6} (\mathbb{1}_2 - 2\omega^{-1} t_r^+ - 2\omega t_r^-) \otimes s_r^z \right) P_r, \end{aligned} \quad (\text{B9})$$

$$\begin{aligned} P_r S_{r,3}^+ P_r &= P_r \begin{pmatrix} 0 & 1/3\sqrt{2} & 0 & 0 & -\sqrt{2}\omega^{-1}/3 & 0 \\ 0 & 0 & 1/3\sqrt{2} & 0 & 0 & -\sqrt{2}\omega^{-1}/3 \\ 0 & 0 & 0 & 0 & 0 & 0 \\ 0 & -\sqrt{2}\omega/3 & 0 & 0 & 1/3\sqrt{2} & 0 \\ 0 & 0 & -\sqrt{2}\omega/3 & 0 & 0 & 1/3\sqrt{2} \\ 0 & 0 & 0 & 0 & 0 & 0 \end{pmatrix} P_r \\ &= P_r \left(\frac{1}{6} (\mathbb{1}_2 - 2\omega^{-1} t_r^+ - 2\omega t_r^-) \otimes s_r^+ \right) P_r. \end{aligned} \quad (\text{B10})$$

Repeating the same procedure for $n = 1$ and 2, we obtain

$$P_r \mathbf{S}_{r,n} P_r = P_r \left(\frac{1}{6} (\mathbb{1}_2 - 2\omega^{n-1} t_r^+ - 2\omega^{-(n-1)} t_r^-) \otimes \mathbf{s}_r \right) P_r, \quad (\text{B11})$$

for $n = 1, 2, 3$. This pseudospin representation of $\mathbf{S}_{r,n}$ reproduces that of \mathbf{T}_r [Eq. (B7)].

Finally, we show how the time reversal T and the $2\pi/3$ rotation R_r looks like in the language of \mathbf{s}_r and \mathbf{t}_r .

$$\begin{aligned} P_r \mathcal{T} P_r &= P_r \begin{pmatrix} 0 & 0 & 0 & 0 & 0 & 1 \\ 0 & 0 & 0 & 0 & 1 & 0 \\ 0 & 0 & 0 & 1 & 0 & 0 \\ 0 & 0 & 1 & 0 & 0 & 0 \\ 0 & 1 & 0 & 0 & 0 & 0 \\ 1 & 0 & 0 & 0 & 0 & 0 \end{pmatrix} P_r \\ &= P_r \left(2t_r^x \otimes [2(s_r^x)^2 - \mathbb{1}_3] \right) P_r \\ &= P_r \left(-2t_r^x \otimes \exp(i\pi s_r^x) \right) P_r, \end{aligned} \quad (\text{B12})$$

$$\begin{aligned} P_r R_r P_r &= P_r \begin{pmatrix} \omega & 0 & 0 & 0 & 0 & 0 \\ 0 & \omega & 0 & 0 & 0 & 0 \\ 0 & 0 & \omega & 0 & 0 & 0 \\ 0 & 0 & 0 & \omega^{-1} & 0 & 0 \\ 0 & 0 & 0 & 0 & \omega^{-1} & 0 \\ 0 & 0 & 0 & 0 & 0 & \omega^{-1} \end{pmatrix} P_r \\ &= P_r \left(\exp\left(i\frac{4\pi}{3} t_r^z\right) \otimes \mathbb{1}_3 \right) P_r. \end{aligned} \quad (\text{B13})$$

- [1] D. J. Thouless, M. Kohmoto, M. P. Nightingale, and M. den Nijs, Quantized hall conductance in a two-dimensional periodic potential, *Phys. Rev. Lett.* **49**, 405 (1982).
- [2] C. L. Kane and E. J. Mele, Z_2 topological order and the quantum spin hall effect, *Phys. Rev. Lett.* **95**, 146802 (2005).
- [3] A. P. Schnyder, S. Ryu, A. Furusaki, and A. W. W. Ludwig, Classification of topological insulators and superconductors in three spatial dimensions, *Phys. Rev. B* **78**, 195125 (2008).
- [4] X. Chen, Z.-C. Gu, Z.-X. Liu, and X.-G. Wen, Symmetry protected topological orders and the group cohomology of their symmetry group, *Phys. Rev. B* **87**, 155114 (2013).
- [5] Z.-C. Gu and X.-G. Wen, Tensor-entanglement-filtering renormalization approach and symmetry-protected topological order, *Phys. Rev. B* **80**, 155131 (2009).
- [6] S. Matsuura, P.-Y. Chang, A. P. Schnyder, and S. Ryu, Protected boundary states in gapless topological phases, *New Journal of Physics* **15**, 065001 (2013).
- [7] T. Scaffidi, D. E. Parker, and R. Vasseur, Gapless Symmetry-Protected Topological Order, *Phys. Rev. X* **7**, 041048 (2017).
- [8] B. Hetényi, Interaction-driven polarization shift in the $t-v-V'$ lattice fermion model at half filling: Emergent haldane phase, *Phys. Rev. Research* **2**, 023277 (2020).
- [9] R.-B. Wang, A. Furusaki, and O. A. Starykh, Majorana end states in an interacting quantum wire, *Phys. Rev. B* **102**, 165147 (2020).
- [10] R. Thorngren, A. Vishwanath, and R. Verresen, Intrinsically gapless topological phases, *Phys. Rev. B* **104**, 075132 (2021).
- [11] Y. He, D. Pekker, and R. S. K. Mong, One-dimensional repulsive hubbard model with mass imbalance: Orders and filling anomaly, *Phys. Rev. B* **104**, 195126 (2021).
- [12] R. Verresen, R. Thorngren, N. G. Jones, and F. Pollmann, Gapless topological phases and symmetry-enriched quantum criticality, *Phys. Rev. X* **11**, 041059 (2021).
- [13] Y. Hidaka, S. C. Furuya, A. Ueda, and Y. Tada, Gapless symmetry-protected topological phase of quantum antiferromagnets on anisotropic triangular strip, *arXiv preprint arXiv:2205.15525* (2022).
- [14] S. C. Furuya and M. Oshikawa, Symmetry Protection of Critical Phases and a Global Anomaly in 1 + 1 Dimensions, *Phys. Rev. Lett.* **118**, 021601 (2017).
- [15] C.-T. Hsieh, O. M. Sule, G. Y. Cho, S. Ryu, and R. G. Leigh, Symmetry-protected topological phases, generalized Laughlin argument, and orientifolds, *Phys. Rev. B* **90**, 165134 (2014).
- [16] P. Calabrese and J. Cardy, Entanglement entropy and quantum field theory, *Journal of Statistical Mechanics: Theory and Experiment* **2004**, P06002 (2004).
- [17] I. Affleck and A. W. W. Ludwig, Universal noninteger “ground-state degeneracy” in critical quantum systems, *Phys. Rev. Lett.* **67**, 161 (1991).
- [18] N. Laflorencie, E. S. Sørensen, M.-S. Chang, and I. Affleck, Boundary Effects in the Critical Scaling of Entanglement Entropy in 1D Systems, *Phys. Rev. Lett.* **96**, 100603 (2006).
- [19] T. Giamarchi, *Quantum Physics in One Dimension* (Oxford University Press, Oxford, 2004).
- [20] H. Watanabe, Y. Kato, H. C. Po, and Y. Motome, Fractional corner magnetization of collinear antiferromagnets, *Phys. Rev. B* **103**, 134430 (2021).
- [21] F. Haldane, Continuum dynamics of the 1-D Heisenberg antiferromagnet: Identification with the O(3) nonlinear sigma model, *Physics Letters A* **93**, 464 (1983).
- [22] F. D. M. Haldane, Nonlinear Field Theory of Large-Spin Heisenberg Antiferromagnets: Semiclassically Quantized Solitons of the One-Dimensional Easy-Axis Néel State, *Phys. Rev. Lett.* **50**, 1153 (1983).
- [23] I. Affleck, Quantum spin chains and the Haldane gap, *Journal of Physics: Condensed Matter* **1**, 3047 (1989).
- [24] F. Pollmann, A. M. Turner, E. Berg, and M. Oshikawa, Entanglement spectrum of a topological phase in one dimension, *Phys. Rev. B* **81**, 064439 (2010).
- [25] F. Pollmann, E. Berg, A. M. Turner, and M. Oshikawa, Symmetry protection of topological phases in one-dimensional quantum spin systems, *Phys. Rev. B* **85**, 075125 (2012).
- [26] H. Tasaki, *Physics and Mathematics of Quantum Many-Body Systems* (Springer International Publishing, 2020).
- [27] I. Affleck, T. Kennedy, E. H. Lieb, and H. Tasaki, Rigorous results on valence-bond ground states in antiferromagnets, *Phys. Rev. Lett.* **59**, 799 (1987).
- [28] S. C. Furuya and M. Sato, Quantized edge magnetizations and their symmetry protection in one-dimensional quantum spin systems, *Phys. Rev. B* **104**, 184401 (2021).
- [29] T. Tonegawa, K. Okamoto, H. Nakano, T. Sakai, K. Nomura, and M. Kaburagi, Haldane, Large- D , and Intermediate- D in $S - 2$ Quantum Spin Chain with On-Site and XXZ Anisotropies, *Journal of the Physical Society of Japan* **80**, 043001 (2011).
- [30] H. Kawamura, Universality of phase transitions of frustrated antiferromagnets, *Journal of Physics: Condensed Matter* **10**, 4707 (1998).
- [31] K. Okunishi, M. Sato, T. Sakai, K. Okamoto, and C. Itoi, Spin-chirality separation and S_3 symmetry breaking in the magnetization plateau of the quantum spin tube, *Phys. Rev. B* **85**, 054416 (2012).
- [32] P. Francesco, P. Mathieu, and D. Sénéchal, *Conformal field theory* (Springer Science & Business Media, 2012).
- [33] E. Lieb, T. Schultz, and D. Mattis, Two soluble models of an antiferromagnetic chain, *Annals of Physics* **16**, 407 (1961).
- [34] I. Affleck, Spin gap and symmetry breaking in CuO_2 layers and other antiferromagnets, *Phys. Rev. B* **37**, 5186 (1988).
- [35] M. Oshikawa, Commensurability, Excitation Gap, and Topology in Quantum Many-Particle Systems on a Periodic Lattice, *Phys. Rev. Lett.* **84**, 1535 (2000).
- [36] M. B. Hastings, Lieb-Schultz-Mattis in higher dimensions, *Phys. Rev. B* **69**, 104431 (2004).
- [37] I. Affleck and E. H. Lieb, A proof of part of haldane’s conjecture on spin chains, *Letters in Mathematical Physics* **12**, 57 (1986).
- [38] M. B. Hastings, Sufficient conditions for topological order in insulators, *Europhysics Letters (EPL)* **70**, 824 (2005).
- [39] M. Oshikawa, M. Yamanaka, and I. Affleck, Magnetization Plateaus in Spin Chains: “Haldane Gap” for Half-Integer Spins, *Phys. Rev. Lett.* **78**, 1984 (1997).

- [40] M. Oshikawa, Insulator, conductor, and commensurability: A topological approach, *Phys. Rev. Lett.* **90**, 236401 (2003).
- [41] G. Y. Cho, C.-T. Hsieh, and S. Ryu, Anomaly manifestation of lieb-schultz-mattis theorem and topological phases, *Phys. Rev. B* **96**, 195105 (2017).
- [42] H. Watanabe, H. C. Po, A. Vishwanath, and M. Zaletel, Filling constraints for spin-orbit coupled insulators in symmorphic and nonsymmorphic crystals, *Proceedings of the National Academy of Sciences* **112**, 14551 (2015).
- [43] M. Cheng, Fermionic lieb-schultz-mattis theorems and weak symmetry-protected phases, *Phys. Rev. B* **99**, 075143 (2019).
- [44] Y. Yao, C.-T. Hsieh, and M. Oshikawa, Anomaly Matching and Symmetry-Protected Critical Phases in $SU(N)$ Spin Systems in $1+1$ Dimensions, *Phys. Rev. Lett.* **123**, 180201 (2019).
- [45] Y. Ogata and H. Tasaki, Lieb–Schultz–Mattis Type Theorems for Quantum Spin Chains Without Continuous Symmetry, *Communications in Mathematical Physics* **372**, 951 (2019).
- [46] Y. Yao and M. Oshikawa, Twisted boundary condition and lieb-schultz-mattis inapplicability for discrete symmetries, *Phys. Rev. Lett.* **126**, 217201 (2021).
- [47] G. 't Hooft, Naturalness, chiral symmetry, and spontaneous chiral symmetry breaking, *NATO Adv. Study Inst. Ser. B Phys.* **59**, 135 (1980).
- [48] A. Kapustin and R. Thorngren, Anomalous discrete symmetries in three dimensions and group cohomology, *Phys. Rev. Lett.* **112**, 231602 (2014).
- [49] Y. Hatsugai, Quantized Berry Phases as a Local Order Parameter of a Quantum Liquid, *Journal of the Physical Society of Japan* **75**, 123601 (2006).
- [50] N. Chepiga, F. Michaud, and F. Mila, Berry phase investigation of spin- S ladders, *Phys. Rev. B* **88**, 184418 (2013).
- [51] X. Chen and A. Vishwanath, Towards gauging time-reversal symmetry: A tensor network approach, *Phys. Rev. X* **5**, 041034 (2015).
- [52] T. Kariyado, T. Morimoto, and Y. Hatsugai, Z_N Berry Phases in Symmetry Protected Topological Phases, *Phys. Rev. Lett.* **120**, 247202 (2018).
- [53] I. Maruyama and S. Miyahara, Fractionally Quantized Berry Phases of Magnetization Plateaux in Spin-1/2 Heisenberg Multimer Chains, *Journal of the Physical Society of Japan* **87**, 123703 (2018).
- [54] S. C. Furuya and Y. Horinouchi, Translation constraints on quantum phases with twisted boundary conditions, *Phys. Rev. B* **100**, 174435 (2019).
- [55] M. A. Metlitski and R. Thorngren, Intrinsic and emergent anomalies at deconfined critical points, *Phys. Rev. B* **98**, 085140 (2018).